JOURNAL OF MATERIALS SCIENCE 20 (1985) 2093–2102

Relaxation processes and pure shear stress creep in a metallic glass ribbon of composition $(Fe_{0.05}Co_{0.95})_{75}Si_{15}B_{10}$

A. HERNANDO*, O. V. NIELSEN
Department of Electrophysics, The Technical University of Denmark, DK-2800 Lyngby, Denmark

V. MADURGA
Laboratory of Magnetism, University Complutense, Madrid-3, Spain

The effect of annealing time and temperature and of pre-annealing on the creep properties of metallic $(Fe_{0.05}Co_{0.95})_{75}Si_{15}B_{10}$ glass ribbons has been studied. The creep strains, measured in a torsional creep mode, can be well interpreted using the concept of an activation energy spectrum. Observed $\ln t$ kinetics as well as deviations from this are comprehensible by considering the form of the characteristic annealing function.

1. Introduction

The mechanical behaviour of amorphous metallic glasses has been studied extensively in recent years [1]. Emphasis has been given to the atomic mechanism involved in creep [2, 3] and to the stress dependence of homogeneous flow, i.e. the determination of the strain rate sensitivity [4]. From a phenomenological point of view two deformation modes can be distinguished: homogeneous flow occurring at low stress and high temperature and inhomogeneous flow observed at high stress and low temperature [5, 6].

Glassy metallic alloys exhibit three strain components during experiments of homogeneous flow: ideal elasticity (recoverable, instantaneous), anelasticity (recoverable, time-dependent) and plasticity (permanent, time-dependent) [7]. Two important facts are well established from the experimental results: the viscosity $\eta(\eta = \tau/\dot{\gamma}$ where τ is the shear stress and $\dot{\gamma}$ is the time derivative of the shear strain) changes more than five orders of magnitude owing to structural relaxation [8] and it has been found that the viscosity is linear with the test annealing time [9].

It has been pointed out, however, that the dramatic increase in viscosity produced by pre-annealing at high temperature does not affect the observed activation energies. This fact may indicate that during structural relaxation a decrease in the available processes for flow rather than a change in their character occurs [10].

The strong dependence on pre-annealing of the viscosity leads to the conclusion that reproducible creep measurements must be done with "well stabilized" samples, thereby avoiding any structural relaxation effects during the stress annealing test. It has been reported that during measurement of the viscosity as a function of the temperature, the absence of structural relaxation can be verified by returning to the initial (higher) testing temperature and testing for no change from the initial value of the viscosity [7].

The need for a more fundamental understanding of flow in metallic glasses has motivated a variety of stress relaxation and creep measurements. These efforts have recently been of considerable interest for investigators dealing with magnetic properties of metallic glasses. The elastic behaviour of some magnetic amorphous alloys possesses an additional interest arising from the excellent magnetomechanical properties

*Permanent address: Laboratory of Magnetism, University Complutense, Madrid-3, Spain.

0022–2461/85 $03.00 + .12

exhibited for some compositions [11–14]. Furthermore the anelastic and plastic strains have been closely related to the magnetic anisotropies induced in ribbons subjected to stress annealing treatments [15–18].

The present work is divided into two parts. First the experimental results of torsional elastic, anelastic and plastic behaviour of the glass alloy $(Co_{0.95}Fe_{0.05})_{75}Si_{15}B_{10}$ are reported. This alloy belongs to the series of $(Co_xFe_{1-x})_{75}Si_{15}B_{10}$ which has been studied with respect to stress-induced anisotropy [19]. Measurements were carried out on both as-cast and pre-annealed samples at different temperatures for constant annealing time and very low constant shear stress.

In the second part, the results are discussed within the framework of a broad activation energy spectrum. A simple phenomenological model based on that given by Argon and Kuo [20] for creep and generalized by Gibbs *et al.* [21] to structural relaxation, accounts for the overall observed viscoelastic behaviour. The model is able to predict the more remarkable features related to viscosity and creep rate, strain relaxation, and influence of pre-annealing on both creep and structural relaxation.

The major objective of this work, the accumulation and the discussion of mechanical experimental data, is to approach a future explanation of the complex mechanisms giving rise to induced magnetic anisotropy during the viscoelastic flow.

2. Experimental details

2.1. Experimental procedure

Amorphous ribbons with the nominal composition $(Co_{0.95}Fe_{0.05})_{75}Si_{15}B_{10}$ were produced by single roller quenching. The starting master alloy was prepared as described elsewhere [22]. The resulting samples were typically 0.9 mm wide and 17 μm thick. The glassy nature of the ribbons was verified by coercive force and X-ray tests.

Torsional experiments were performed on ribbons of 8 cm length placed in a system for simultaneous magnetic measurements and torsional creep. The details of the apparatus have been reported elsewhere [23]. The heating chamber can keep the sample at constant temperature within ± 1° C over its length. The device supplies a plot of the torsional strain as a function of time. Torsional stress–strain curves at different temperatures can also be plotted automatically.

Creep measurements were carried out under the following conditions: the ribbons were heated from room temperature to the stress-annealing temperature, T_{ann}, and held at this temperature for 6 min after which time a constant torque was applied, producing an instantaneous torsion angle per unit length (angular elastic strain) $\xi_{el}(T_{ann})$. The flow was monitored during the whole creep process which always was of 120 min duration. During the stress-annealing process the total strain ξ_{tot} can be expressed

$$\xi_{tot}(T_{ann},t) = \xi_{el}(T_{ann}) + \xi_c(T_{ann},t) \quad (1)$$

where $\xi_c(T_{ann},t)$ is the time-dependent creep strain. Keeping the applied torque fixed, the sample was cooled down to room temperature and then the torque was removed.

The instantaneous restoring strain, $\xi_{el}(T_r,T_{ann})$, observed at room temperature, when the sample is relieved, was measured. In order to determine the anelastic strain component, the ribbons were reheated without applied torque to the corresponding T_{ann} for a period of 120 min. The time-dependent relaxing strain, $\xi_{re}(T_{ann},t)$, was plotted during the whole process, after which the remanent strain, $\xi_p(T_{ann}, 120\text{ min})$, was measured.

The creep strain can now be split up into two components

$$\xi_c(T_{ann}, 120\text{ min}) = \xi_{an}(T_{ann}, 120\text{ min}) + \xi_p(T_{ann}, 120\text{ min}) \quad (2)$$

where

$$\xi_{an}(T_{ann}, 120\text{ min}) = -\xi_{re}(T_{ann}, 120\text{ min})$$

For the experiments reported here, T_{ann} ranges from 516 to 672 K. Tests were performed for as-cast as well as for pre-annealed samples. The preannealing conditions were $\overline{T}_p = 673$ K and $t_p = 120$ min. All the creep experiments were performed with the same strength of the applied torque which produced a maximum shear stress, τ, occurring at the ribbon surfaces, of 163 MPa. The experimental data reported for the strain are given for the shear strain, γ, at the ribbon surfaces. For details of converting applied torque and torsion angle per unit length into shear stress and strain, respectively, see [14]. The heating and cooling rates were 35 and 10 K min^{-1}, respectively.

The crystallization temperature of the glass alloy was 763 K, tested by using a heating rate of 5 K min^{-1}.

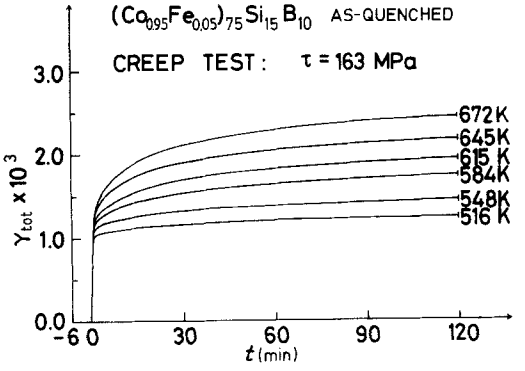

Figure 1 Torsional creep curves for as-quenched ribbons.

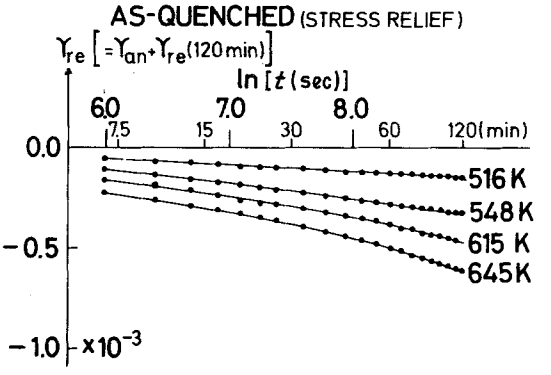

Figure 3 Strain relaxation for as-quenched ribbons, measured after 120 min stress annealing.

2.2. Experimental results

Fig. 1 shows the total strain, $\gamma_{tot}(T_{ann},t)$ as a function of the annealing time, of as-cast samples creep tested at different temperatures. The strain increases linearly with the logarithm of time as illustrated in Fig. 2.

The strain relaxation processes of these samples are plotted in Fig. 3. It is clearly true that a linear behaviour of $\gamma_{an}(T_{ann},t)$ $(=\gamma_{re}(T_{ann},t)-\gamma_{re}$ $(T_{ann}$, 120 min) with the logarithm of the strain relaxation annealing time does not occur.

The different components of the strain defined above are depicted in Fig. 4 as a function of the annealing temperature. From Fig. 4 it is evident that γ_p is larger than γ_{an} at all the temperatures tested. At the lower temperatures γ_p and γ_{an} rise with a similar rate but from $T_{ann} \sim 560$ K they exhibit quite different behaviour. While γ_p increases rapidly with increasing T_{ann}, γ_{an} shows a slow increase and finally attains a saturation value of approximately 0.62×10^{-3}.

It is reasonable to examine the evolution with the temperature of the two elastic strain components: $\gamma_{el}(T_{ann})$ (not shown in Fig. 4) reveals a slow increase with increasing T_{ann}, ranging from 1.1 to 1.4×10^{-3} at $T_{ann} = 576$ and 672 K, respectively, while $\gamma_{el}(T_r,T_{ann})$, measured at room temperature when removing the torque, decreases drastically with increasing T_{ann}, from 0.83×10^{-3} for $T_{ann} = 516$ K, to 0.32×10^{-3} for $T_{ann} = 672$ K. Considering the value of the shear modulus determined at room temperature for as-cast samples $\mu(T_r) = 89$ GPa, the observed variation of $\gamma_{el}(T_r,T_{ann})$ would signify an increase of $\mu(T_r)$ of around 150%. It must be added that such a giant variation cannot be explained exclusively as a consequence of the structural relaxation. Moreover, measurements of the shear modulus of pre-annealed samples with no applied stress yield for μ a value of 104 GPa. The unbiased structural relaxation rise of μ of 17% is in good

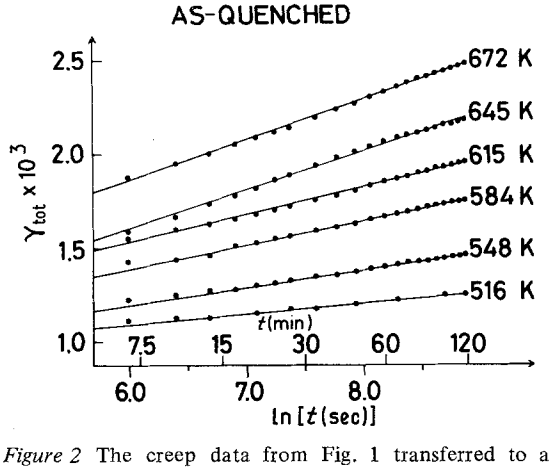

Figure 2 The creep data from Fig. 1 transferred to a logarithmic time scale.

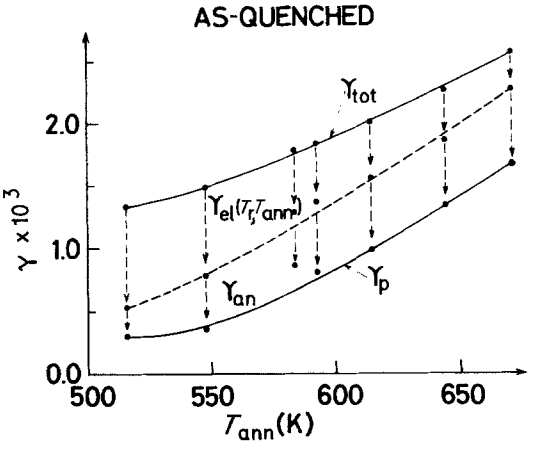

Figure 4 As-quenched ribbons. Plastic strain γ_p and anelastic strain γ_{an} after 120 min stress annealing. The elastic strains $\gamma_{el}(T_r,T_{ann})$ were measured at room temperature after the stess annealing treatments.

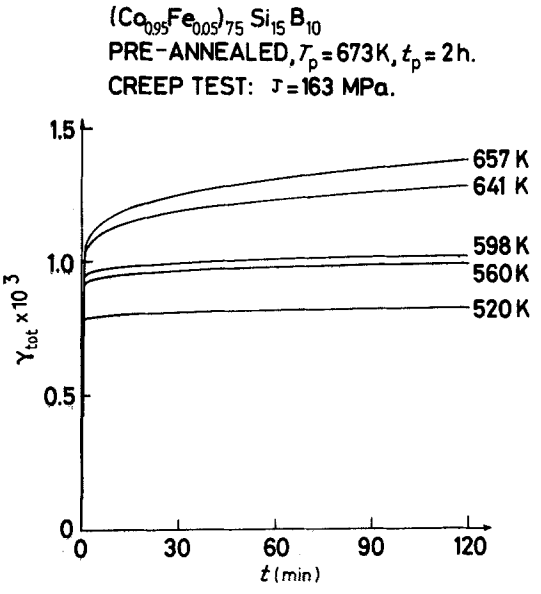

Figure 5 Torsional creep curves for pre-annealed ribbons.

agreement with previous reported results for other compositions [24–27].

The smooth dependence on T_{ann} of $\gamma_{el}(T_{ann})$ is not surprising and shall be analysed as a combination of two competitive processes: the thermal dependence of the elastic constants and the structural relaxation achieved from the beginning of the heating process to the time when the torque is applied.

Hitherto we have described the more remarkable features of the behaviour of as-cast samples. Figs. 5 and 6 show the creep tests of pre-annealed ribbons. A true linear behaviour in $\ln t$ with a small slope is observed for low annealing temperatures. It is to be noticed, however, that the slopes

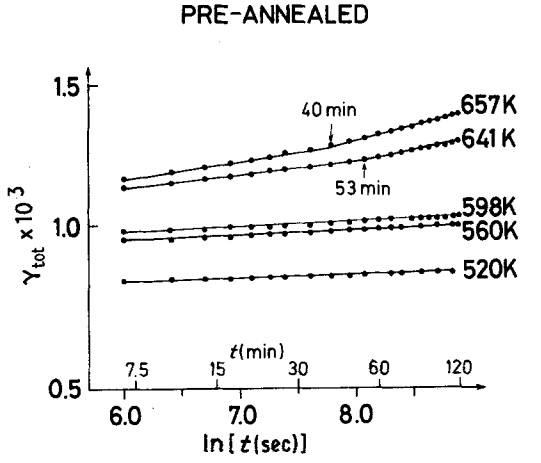

Figure 6 The creep data from Fig. 5 transferred to a logarithmic time scale.

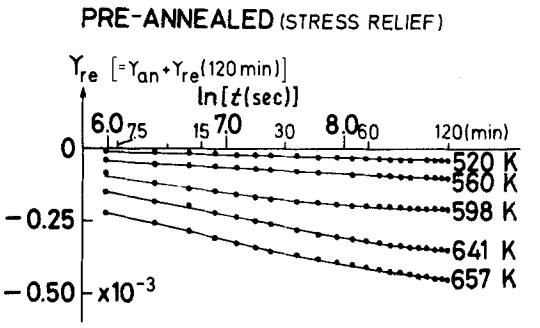

Figure 7 Strain relaxation for pre-annealed ribbons, measured after 120 min stress annealing.

exhibit a remarkable increase with increasing T_{ann} from ~ 600 K. As was expected, the isothermal strain rates of pre-annealed ribbons are significantly lower than those observed for as cast samples.

The strain relaxation kinetics does not obey a "ln t" law at the higher temperatures where a trend to decrease the strain relief rate with increasing ln t is evident. Nevertheless, at the lower temperatures the strain relaxation can be approximated by a ln t law as shown in Fig. 7.

Fig. 8 illustrates the behaviour of the different experimental components of the strain as a function of T_{ann} for pre-annealed samples. As can be observed, γ_{an} remains higher than γ_p for all the temperatures. At the lower temperatures, γ_p is very low but it rises, with progressively increasing rate, from $T_{ann} \sim 600$ K.

$\gamma_{el}(T_r, T_{ann})$ is roughly constant for $T_{ann} < 600$ K, but shows a strong decrease for higher annealing temperatures, where it becomes 0.3 γ_{el} (T_{ann}), approximately.

$\gamma_{el}(T_{ann})$ shows a typical dependence of the

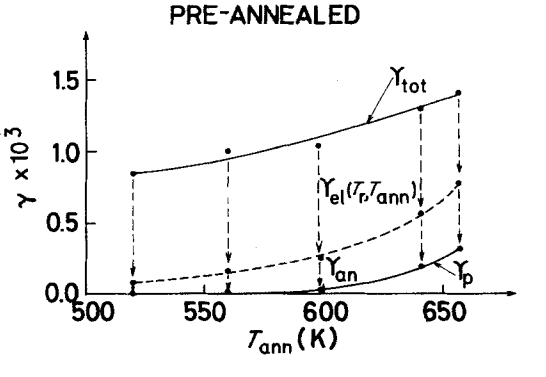

Figure 8 Pre-annealed ribbons. Plastic strain γ_p and anelastic strain γ_{an} after 120 min stress annealing. The elastic strains $\gamma_{el}(T_r, T_{ann})$ were measured at room temperature after the stress annealing treatments.

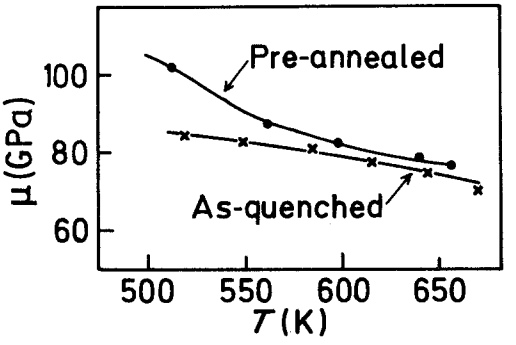

Figure 9 Temperature dependence of the shear modulus μ for as-quenched and for pre-annealed ribbons.

elastic constants on the temperature as plotted in Fig. 9, where the structural relaxation effect on the shear modulus is evident.

It may be worthwile to remark that the observed change of the shear modulus after stress-annealing is high enough, even for the pre-annealed ribbons, to be explained as a consequence of the structural relaxation (i.e. $\Delta\mu/\mu = 20\%$ for $T_{ann} = 657$ K).

A creep process fitting a $\ln t$ kinetics leads to a linear dependence on time of the viscosity, which is defined as $\eta = \tau/\dot{\gamma}$. The linear dependence of the viscosity with time found from the experimental results is plotted in Fig. 10.

3. Data analysis

3.1. Phenomenological model

The creep tests exhibit an excellent linear behaviour of the strain with the logarithm of the isothermal annealing time. This phenomenon has been commonly observed in previous studies of relaxation in amorphous alloys [24–28]. It has recently been pointed out by Gibbs *et al.* [21] that the measured properties change linearly with the logarithm of time when the atomic processes contributing to the observed change exhibit a "broad" spectrum of activation energies. Moreover, they have developed a model, based upon this idea, which accounts in general for the more commonly reported features of the structural relaxation in metallic glasses. It is worth noting that before this cited model was achieved, Argon and Kuo [20] considered a spectrum of activation energies to understand some experimental results concerning anelastic load relaxation in metallic glasses. Therefore the analysis of the experimental data reported here shall be carried out by assuming that the atomic processes contributing to the strain exhibit a wide spectrum of activation

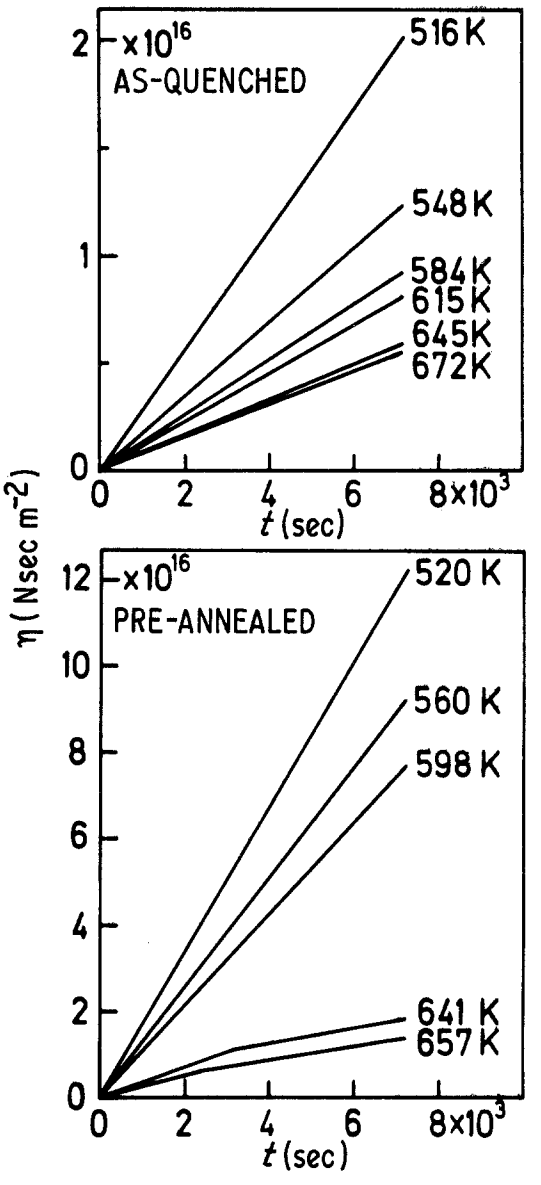

Figure 10 Viscosity η as a function of time for as-quenched and for pre-annealed ribbons.

energies. Of particular interest is a clearer understanding of the evolution of the total number of processes available for strain after the different thermal treatments labelled pre-annealing, stress annealing, and strain relaxation.

It is assumed that the bias effect exerted on the activated processes by the applied stress is given by the well established law of $\sinh(\tau\gamma_o\Omega_f/kT)$ where γ_o is the local strain produced by a shear site of volume Ω_f. We need to consider only the small stress limit [4] where

$$\sinh\left(\frac{\tau\gamma_o\Omega_f}{kT}\right) \approx \frac{\tau\gamma_o\Omega_f}{kT} \qquad (3)$$

Following the ideas outlined in [21] we introduce the number densities $q_s(E)$ and $q(E)$ of available processes. Here $q_s(E)$ is the equilibrium number density of available processes contributing to the strain while $q(E)$ is the excess (or deficit) of available processes as compared to the equilibrium density, $q_s(E)$. Note that $q_s(E)$ must be an increasing function with increasing temperature [21].

Furthermore it is assumed that the rate of activation of the flow units with activation energy E is governed by first-order reaction kinetics, so that the total number density of such processes activated after time t at a temperature T will be

$$Q_t(E) = Q(E)\theta(E,T,t) \quad (4)$$

where $Q(E)$ is the total available number density at $t = 0$, $(Q = q + q_s)$ and where

$$\theta(E,T,t) = 1 - \exp\left[-\nu_o t \exp\left(\frac{-E}{kT}\right)\right] \quad (5)$$

ν_o being the frequency factor of the process.

These assumptions allow us to express tentatively the isothermal strain [20] as:

$$\gamma(\tau,T,t) = \frac{\tau}{kT}\int_0^\infty c(E)Q(E)\theta(E,T,t)\mathrm{d}E \quad (6)$$

where $c(E)$ is the average value of $\Omega_f\gamma_o$ for all the processes with activation energy between E and $E + \mathrm{d}E$.

The more remarkable features of $\theta(E,T,t)$ have been pointed out by Gibbs *et al.* [21] and they are: θ changes from 0.01 to 0.99 over a narrow range, δE, and it can be considered as centered at

$$E_o = kT\ln(\nu_o t) \quad (7)$$

According to Equation 7 it is easy to find the energy range ΔE swept during an isothermal treatment. It is clear that if $c(E)Q(E) \simeq$ constant over ΔE, Equation 6 leads to a $\ln t$ law:

$$\gamma(\tau,T,t) = \tau < c(E)Q(E) > \ln(\nu_o t) \quad (8)$$

where $< c(E)Q(E) >$ is the mean value averaged over ΔE (i.e. $\ln(t/t_i)$, t_i being the isothermal time at which the torque is applied).

This peculiar time dependence yields for the viscosity

$$\eta = \frac{t}{< c(E)Q(E) >} \quad (9)$$

It is to be expected that after pre-annealing, a fraction of processes $q(E)$ will disappear by irreversible unbiased activation, thus producing the commonly reported increase of the viscosity during a subsequent stress-annealing test.

3.2. Experimental results

Considering $\nu_0 = 10^{12}$ sec^{-1} as the Debye frequency for a single process, the energy range ΔE tested during the isothermal treatments reported in Section 2 can be derived from Equation 7. ΔE is typically 0.15 eV. The total interval studied ranges between 1.5 to 2.1 eV.

3.2.1. As-quenched ribbons

The creep processes exhibited by as-cast samples confirm that $c(E)Q(E)$ can be considered constant during each isothermal process, although it increases with increasing T_{ann}. Fig. 11 shows a tentative spectrum profile found from the slopes of the straight lines of Fig. 2, by using Equation 8.

It must be noticed that the total number of activated processes during an isothermal creep test is $\Delta EQ(E)$ where it is assumed that θ is a step function. This is a reasonable approximation when the variation of $Q(E)$ is negligible due to the variation range, δE, of θ. The total number of processes available for activation on a subsequent sweeping of the same ΔE will have decreased to $q_s(E)\Delta E$ since the difference is the number of processes irreversibly activated during the first treatment. Comparing the slopes for the as-quenched specimen (Fig. 2) with those for the pre-annealed specimen (Fig. 6) we find that $Q(E) \gg$

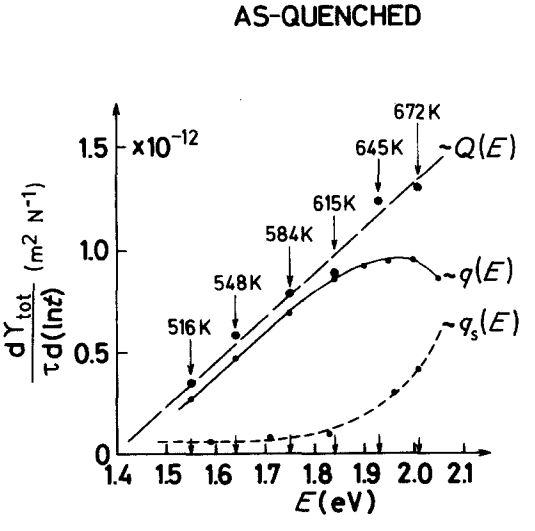

Figure 11 Tentative number density profile $< c(E)Q(E) > = \mathrm{d}\gamma_{tot}/\gamma d(\ln t)$ for as quenched ribbons, calculated from the creep data in Fig. 2. $q_s(E)$ depends on T and the plotted values correspond to the T_{ann} values indicated.

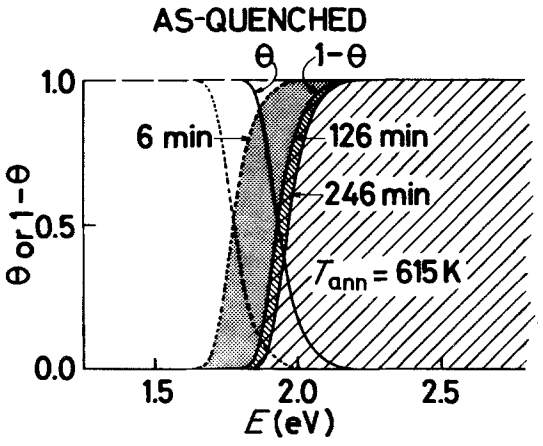

Figure 12 As-quenched ribbons. Evolution with time of the number density function $q(E)$ putting $q(E) = 1$ at $t = 0$. ▨ processes not activated; ⊡ processes activated during stress annealing; ▧ processes activated during stress relief.

$q_s(E)$ for most of the energy range swept. The first stress annealing produces a biased contribution from the structural relaxation to the total strain. This contribution is essentially the same as the one arising from thermal generation of processes (i.e. coming from processes of type $q_s(E)$) but it differs in the following sense: if the sample is reheated with no applied stress to the same temperature for the same time, then the total number of processes available to be biased by the back stresses, thus contributing to the strain relaxation, becomes $q_s(E) < Q(E)$. Therefore they cannot remove all the strain, even in the presence of restoring stresses, thereby explaining the appearance of a residual plastic strain due to the structural relaxation.

Fig. 12 illustrates the profile for irreversible processes after the stress annealing and the effect produced on it during the subsequent process of strain relaxation. θ has not been approximated to a step function because the basis for this approximation breaks down. Actually the profile of $q(E)$ after the first annealing is identical to $1 - \theta$. As shown in the figure, some irreversible processes of higher energy are activated during the strain relaxation and its number increases with increasing time. This behaviour could account for the progressive increase of rate observed in Fig. 3. It has been calculated that the total number of irreversible processes available for strain relaxation is approximately 0.3 times the number of such processes contributing to the strain during the stress annealing. This suggests that both strain components γ_p and γ_{an} must rise with similar rate with increasing T_{ann} if the same relative back stresses are assumed. Nevertheless a trend to saturation is shown by γ_{an} (Fig. 4) from $T_{ann} \sim 560$ K. This seems to indicate that back stresses are approaching a saturation value. (We will ignore here the microscopic mechanisms giving rise to the strain but for details see the model given by Argon and Shi [29] and Srolovitz *el al.* [3]).

Finally it must be added that the giant change exhibited by the shear modulus (Fig. 4) could be due to the "biased" structural relaxation which would give rise to a strong elastic anisotropy. Some experiments dealing with this phenomenon will be reported as soon as possible.

3.2.2. Pre-annealed ribbons

In order to predict the behaviour of samples pre-annealed with no stress, before the creep test, it is required to know the influence exerted by the thermal treatment on the shape of $Q(E)$. The final E_0 reached with the pre-annealing condition reported in Section 2 was 2.1 eV. If θ is assumed to be a step function, only a contribution from processes of type $q_s(E)$ would be expected for stress annealing tests with final $E_0 < 2.1$ eV. In this case the basis for the step function approximation also breaks down. Fig. 13 shows the profile of the spectrum for irreversible processes after 120 min pre-annealing at 673 K. It is clear that for a 120 min thermal treatment at 598 K some amount of irreversible processes are activated. According to that a negligible

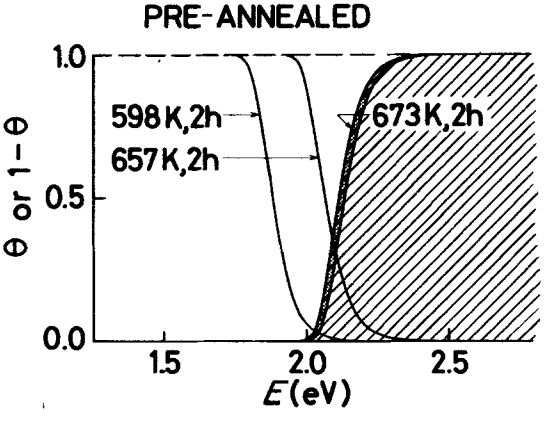

Figure 13 Illustrates the effect of 2 h pre-annealing at 673 K on the number of activated irreversible processes in a subsequent creep experiment at 598 or 657 K. ▨ processes not activated.

contribution from the structural relaxation should be expected only for the lower T_{ann}, i.e. 520 and 560 K. The creep behaviour experiments show an overall consistency with these predictions. If the $\ln t$ kinetics observed for the lower T_{ann} is due to processes of type $q_s(E)$, then the same number of defects can contribute to the strain relaxation. Hence $\gamma_{an} = \gamma_c$, indicating that for low strains the back stresses are proportional to γ_c, and γ_p tends to zero. The absence of "biased" structural relaxation accounts for $\gamma_{el}(T_{ann}) \simeq \gamma_{el}(T_r, T_{ann})$. The strain relaxation curves reach a saturation value when the back stresses relieve as γ_c decreases (Fig. 7).

With increasing T_{ann}, structural relaxation starts to contribute as illustrated by Fig. 13. As a natural consequence, the creep rises during the isothermal annealing and γ_p increases while $\gamma_{el}(T_r, T_{ann})$ decreases. The curves plotted in Fig. 7 for the higher temperatures show initially an analogous trend to the one exhibited for lower temperatures but finally they do not reach a saturation value. This behaviour can be explained as in the case of as-cast samples: it is the new processes irreversibly activated during the strain relaxation annealing which contribute to the reversibility of the macroscopic property.

It must be added that by extrapolating to zero the anelastic strain experimentally determined, the threshold activation energies for detecting creep were found to be 1.2 and 1.44 eV for as-cast and pre-annealed samples, respectively. It is a reasonable result which indicates that the lower the activation energy is, the higher is the difference between $q(E)$ and $q_s(E)$. Note that $q_s(E)$ should be identical to $Q(E)$ at the fictive temperature of the glass.

4. Discussion

The experimental results reported here show an overall consistency with the model based on a spectrum of activation energies. Therefore the discussion will be based within this framework. We wish to remark that the phenomenological model considered here only accounts for the processes available for strain as a function of the thermal treatment carried out before, during and after the creep test. We will ignore the microscopic models and the stress influence on the strain-rate. The discussion will be centered around two subjects: Influence of pre-annealing on the strain-rate and on the total strain.

4.1. Influence of pre-annealing on the strain-rate

From the literature about creep properties it can be seen that particular emphasis has been given to the need for pre-annealing in order to avoid the influence of structural relaxation on the strain-rate.

The model based on a spectrum of activation energies can be used to determine the changes introduced in $q(E)$ by pre-annealing. It has been found that in subsequent annealings the structural relaxation can start at temperatures approximately 100 K below the pre-annealing temperature. If the total number density $Q(E) = q(E) + q_s(E)$ for available processes is known, the spectrum $Q'(E)$ after pre-annealing can be obtained by applying the relation:

$$Q'(E) = Q(E) - q(E)\,\theta(E, T_p, t_p) \qquad (10)$$

where the function θ (Equation 5) must be taken at the pre-annealing conditions T_p and t_p.

The creep rate observed for as-cast samples is expected to be proportional to $1/t$, hence the viscosity should be proportional to the annealing time as many authors have found previously. The mean value of $c(E)Q(E)$ averaged in the energy range corresponding to each isothermal treatment can be obtained from the slopes of the straight lines obtained by plotting the strain as a function of $\ln t$.

Theory predicts and experiments confirm that a linear behaviour of the strain with the logarithm of time, i.e. $1/t$ creep rate, is obtained for pre-annealed samples at $T_{ann} \ll T_p$. This behaviour breaks down when the function $\theta(E, T_{ann}, t_{ann})$ overlaps the function $1 - \theta(E, T_p, t_p)$. At this point deviations from $\ln t$ behaviour can be observed because structural relaxation starts to contribute. This fact could explain the creep results reported by Argon and Kuo [20] for a single T_{ann} 50 K below T_p.

It is to be noted that the model used here leads to the following conclusion for a pre-annealed ribbon: the absence of structural relaxation during an experiment at a high temperature cannot be checked by comparing the viscosities measured at a lower temperature before and after the high temperature experiment.

4.2. Plastic and anelastic strain

The nonrecoverable plastic strain may originate from two different causes:

(a) The number N_r of available processes activated during the strain-relaxation annealing is less than the number N_s activated during the stress-annealing.

(b) The restoring back-stresses do not have sufficient strength to produce a bias effect high enough to remove the remanent strain.

It has been found for as-cast ribbons that $N_r/N_s \simeq 0.3$, therefore an unavoidable plastic strain is always present. The relative value of 0.3 does not change appreciably with T_{ann}. Hence, if it is assumed that the strength of back-stresses is proportional to the creep strain, the anelastic strain would be lower but proportional to the plastic one. It was observed that γ_{an} and γ_p rise at a similar rate with increasing T_{ann} up to $T_{ann} \simeq 560$ K, in the experiments performed with as-cast ribbons. This suggests that the restoring back-stresses are proportional to γ_c in this T_{ann} range. The subsequent drastic increase shown by γ_p, accompanied by a saturation of γ_{an}, indicates the appearance of type (b) mechanisms, contributing to strain and keeping saturated the strength of the back stresses.

In the T_{ann} range where no structural relaxation is expected, the preannealed ribbons do not exhibit any plastic strain. In this range $N_s = N_r$ and the possible contribution from cause (a) cannot be invoked. Plastic strain from the stress-annealing treatment rises from the temperature for which the theory predicts the starting of structural relaxation. Therefore the contribution from cause (a) starts.

It must be pointed out that the appearance of strain contributions from cause (b) does not seem related to a particular activation energy but to the level of the strain (this fact is in good agreement with the model and Argon and Shi [29]). If this is true it leads to the conclusion that homogeneous plastic flow requires the contribution from the structural relaxation in order to reach high strain levels. In this case, as a paradox, the so-called iso-configurational plastic flow should not occur in the range of temperatures for which structural relaxation does not occur in preannealed samples.

5. Conclusions

The application of the model based on a wide spectrum of activation energies [20, 21] to the creep experiments reported here leads in a natural way to an explanation of the most remarkable features of the data as well as of the more common features reported previously. This model seems to be a powerful framework to describe the anomalous creep behaviour observed in metallic glasses, thus providing a link to a microscopic analysis.

In order to account for the influence of thermal history and thermal stress and strain relaxation on the creep phenomena the true shape of $\theta(E,T,t)$ has to be considered. Recently it has been done successfully by Leake *et al.* [30] in explaining crossover and reversibility effecs in metallic glasses and by Gibbs *et al.* [31] in explaining $\ln t$ kinetics in metallic glasses. The different creep rates observed can be understood. The flow observed in pre-annealed ribbons has an expected influence from structural relaxation and no evidence of other causes is obtained.

The only assumption required to apply the model is that the density of processes $Q(E)$ contributing to the strain is a smooth function in the energy range swept during an isothermal test. The reasonability of this assumption is clearly confirmed by the excellent fitting of the experimental strain in as-cast ribbons to the $\ln t$ law.

In order to gain information about the character of the processes it is suggested to monitor simultaneously non-mechanical quantities.

Acknowledgements

The authors wish to express their thanks to Professor S. Velayos for this continued interest and to Professor V. Frank for his critical reading of the manuscript. One of us (AH) gratefully acknowledges the Danish Government for financial support.

References

1. J. C. M. LI, Proceedings of the 4th International Conference on Rapidly Quenced Metals, Sendai, August 1981, Vol. II (The Japan Institute of Metals, Sendai, 1982) p. 1335.
2. A. S. ARGON, *Acta Metall.* **27** (1979) 4758.
3. D. SROLOVITZ, V. VITEK and T. EGAMI, *ibid.* **31** (1983) 335.
4. A. I. TAUB, *ibid.* **30** (1982) 2117.
5. P. S. STEIF, F. SPAEPEN and J. W. HUTCHINSON, *ibid.* **30** (1982) 447.
6. H. KIMURA and T. MASUMOTO, *ibid.* **31** (1983) 231.
7. A. I. TAUB and F. SPAEPEN, *J. Mater. Sci.* **16** (1981) 3087.
8. *Idem, Scripta Metall.* **13** (1979) 195.
9. *Idem, Acta Metall.* **28** (1980) 1781.
10. *Idem, Scripta Metall.* **24** (1980) 1197.

11. H. T. SAVAGE and M. L. SPANO, *J. Appl. Phys.* **53** (1982) 2092.
12. J. D. LIVINGSTON, *Phys. Status Solidi a* **70** (1982) 591.
13. A. HERNANDO and V. MADURGA, *Appl. Phys. Lett.* **43** (1983) 749.
14. A. HERNANDO and J. BARANDIARAN, *Phys. Rev. B* **22** (1980) 2445.
15. O. V. NIELSEN and H. J. V. NIELSEN, *J. Magn. Magn. Mater.* **22** (1980) 21.
16. O. V. NIELSEN, H. J. V. NIELSEN, T. MASUMOTO and H. M. KIMURA, *ibid.* **24** (1981) 88.
17. O. V. NIELSEN, *ibid.* **36** (1983) 81.
18. H. R. HILZINGER, Proceedings of the 4th International Conference on Rapidly Quenched Metals, Sendai, August 1981, Vol. II (The Japan Institute of Metals, Sendai, 1982) p. 791.
19. O. V. NIELSEN, L. K. HANSEN, A. HERNANDO and V. MADURGA, *J. Magn. Magn. Mater.* **36** (1983) 73.
20. A. S. ARGON and H. Y. KUO, *J. Non-Cryst. Solids* **37** (1980) 241.
21. M. R. J. GIBBS, J. E. EVETTS, J. A. LEAKE, *J. Mater. Sci.* **18** (1983) 278.
22. V. MADURGA, E. ASCASIBAR, J. GONZÁLES, M. MORALA, A. GARCIA-ESCORIAL, J. PECES and O. V. NIELSEN, *An. Fis.* **79** (1983) 82.
23. V. MADURGA, A. HERNANDO and O. V. NIELSEN, *J. Phys. E. Sci. Instr.* **17** (1984) 813.
24. M. G. SCOTT, R. W. CAHN, A. KURSUMOVIC, E. GIRT and M. B. NJEHOVIC, Proceedings of the 4th International Conference on Rapidly Quenched Metals, Sendai, August 1981, Vol. I (The Japan Institute of Metals, Sendai, 1982) p. 469.
25. A. KURSUMOVIC, R. W. CAHN and M. G. SCOTT, *Scripta Metall.* **14** (1980) 1245.
26. M. G. SCOTT and A. KURSUMOVIC, *Acta Metall.* **30** (1982) 853.
27. A. HERNANDO, A. GARCIA-ESCORIAL, E. ASCASIBAR and M. VÁZQUES, *J. Phys. D. Appl. Phys.* **16** (1983) 1999.
28. T. EGAMI, *J. Mater. Sci.* **13** (1978) 2587
29. H. S. ARGON and L. T. SHI, *Acta Metall.* **31** (1983) 499.
30. J. A. LEAKE, M. R. J. GIBBS, S. VRYENHOEF and J. E. EVETTS, *J. Non-Cryst. Solids* **61/62** (1984) 787.
31. M. R. J. GIBBS, D. W. STEPHENS and J. E. EVETTS. *ibid.* **61/62** (1984) 925.

Received 16 April
and accepted 31 July 1984